

A Saliency-based Unsupervised Method for Angiectasia Detection in Endoscopic Video Frames

Farah Deeba¹  · Shahed K. Mohammed¹ · Francis M. Bui¹ · Khan A. Wahid¹

Received: 30 August 2016 / Accepted: 20 June 2017 / Published online: 19 July 2017
© Taiwanese Society of Biomedical Engineering 2017

Abstract The detection of angiectasia, the primary suspected lesion in patients with obscure gastrointestinal bleeding, presents a challenging problem for physicians. In this paper, we present a saliency based unsupervised method for automatic localization and detection of angiectasia in wired and capsule endoscopic images. To achieve comparable illumination in images from both modalities, image enhancement based on Retinex is performed on the capsule endoscopic images. A saliency detection algorithm has been proposed where the saliency map is formed from the processed images using two distinctness measures: pattern distinctness and color distinctness. The angiectasia specific saliency detection algorithm is able to highlight the lesion affected areas. An adaptive thresholding is performed based on the saliency peaks detected from the gradient images. The performance of the proposed method is evaluated on a dataset consisting of 3602 images, among which 968 images show the indication of angiectasia. The method achieves very high localization score (95.04%), localization precision, moderate specificity (>80%) and a very low detection latency (<0.2 s) for both imaging modalities. A comparison with state-of-the-art saliency detection methods exhibits the efficacy of proposed saliency detection algorithm for angiectasia localization and detection.

Keywords Angiectasia · Endoscopy · Retinex · Saliency detection · Detection latency

✉ Farah Deeba
farah.deeba@usask.ca

¹ Department of Electrical and Computer Engineering,
University of Saskatchewan, Saskatoon, SK S7N 5A9,
Canada

1 Introduction

Angiectasia, also known as vascular ectasia, angiodysplasia, arteriovenous malformation in literature, is a circumscribed dilation of the capillary vessels in the mucosa or submucosa of the gastrointestinal (GI) tract [1]. Angiectasia is the most common vascular lesion of the GI tract in the general population with the estimated prevalence of 0.9–3% in asymptomatic patients and up to 6% in symptomatic patients [2]. With the advent of imaging technologies enabling direct visualization of GI tract, angiectasia is increasingly recognized as a major cause of GI bleeding, particularly in the elderly. The association of angiectasia with obscure GI bleeding (OGIB) has been evidenced in several studies [3, 4], angiectasia being responsible for 30–40% of overall OGIB cases. Moreover, half of the symptomatic patients with angiectasia experience recurrent bleeding [5]. The difficulties in locating angiectasias, which are commonly small, flat and of transitory nature, significantly degrade quality of life and increase economic burden requiring repeated testing, blood transfusion and frequent hospitalization. Being a common and perplexing pathological condition, the correct localization and identification of angiectasia is of critical significance to the gastroenterologists to initiate required clinical procedure.

Recent studies demonstrate that angiectasia is the most common cause of small intestinal bleeding [5, 6]. However, the most common site of angiectasia is the cecum and ascending colon [7]. In case of evaluating patients with GI bleeding, esophagogastroduodenoscopy (EGD) and colonoscopy are first performed to detect the origin of bleeding in upper intestine and large intestine. These wired endoscopic procedures cannot access the entire small intestine. Therefore, capsule endoscopy is performed if the findings

on EGD and colonoscopy are negative, indicating OGIB [3].

The detection of angiectasia is challenging due to various reasons. Angiectasia is among the commonly overlooked lesions in both upper GI tract and large intestine [3]. Capsule endoscopy, with a higher yield compared to double-balloon enteroscopy and push enteroscopy, is associated with a significant miss rate of 31% in detecting angiectasia. Human error, presence of angiectasia in a small number of frames, minute or subtle appearance of lesions are some of the causes responsible for the significant miss rate of angiectasia. A computer-aided screening and decision making system designed to detect angiectasia can reduce both the burden of manually viewing enormous visual data and miss rate of lesions. There has been a large body of research publications in recent years on the development of computer-aided detection system [8, 9]. These researches are mostly focused to classify the abnormalities into broader categories, for example, bleeding, lesion, ulcer, etc. A more useful approach could be adopted by emphasizing on the development of a dedicated computer aided detection (CAD) system for specific pathologies. Angiectasia is associated with certain risk factors and clinical condition including aging, aortic stenosis, Von Willebrand disease, chronic renal failure, hypertension, cardiovascular diseases, and use of anti-coagulants [6]. In case of patients with GI bleeding presenting with these risk factors, the application of a CAD system particularly designed to detect angiectasia is more logical and expected to achieve better result than the system for the detection of lesions in general. Therefore, in this paper, we have proposed a saliency based unsupervised method dedicated for angiectasia detection in endoscopic images.

Saliency based approaches are being emerging in the field of video endoscopy to detect abnormalities, e.g., bleeding [10, 11], ulcer [12], and neoplastic lesions [13]. A few research works can be found in literature which have addressed the problem of automatic angiectasia detection. In [14], a point saliency based method has been proposed to detect lesions including angiectasia, where area under the receiver-operating characteristic curve ranging from 69.9 to 97.5% has been achieved. The limitation of the point saliency detection method proposed in [14] is that it cannot discriminate between normal and abnormal regions, and select salient points from both regions. An additional stage of classification is required to classify selected salient points, imposing dependence on the size and quality of training data. Contrary to the existing methods, we have designed an unsupervised method by constructing a saliency detection algorithm specific to a particular lesion. The proposed unsupervised method does not require any prior training and consequently the dependence on size and quality of training data are eliminated.

Angiectasia is characterized by flat or slightly elevated, discrete, red, fan-shaped area with delicate, reticular pattern on a background of normal small intestinal mucosa [15], as can be seen in Fig. 1. From the special appearance of angiectasia lesions, they can qualify as visually salient regions in an endoscopic video frame. It should be noted that the lighting condition and contrast are significantly different in wireless capsule endoscopic videos compared to wired endoscopic videos. Therefore, the same algorithm will not be applicable for both modalities. Keeping these facts in mind, we propose a new saliency-based unsupervised angiectasia detection algorithm. One of the major contribution of our work is that the proposed method can be applied for both capsule and wired endoscopic videos. To achieve this, we have applied Retinex based adaptive image enhancement on the capsule endoscopic images. Another important contribution of our work is that the proposed saliency detection algorithm is able to localize angiectasia lesions by detecting significant part of the affected region.

2 Methods

The proposed method consists of three consecutive stages: (1) preprocessing, (2) saliency detection, and (3) adaptive thresholding. An overview of the proposed method has been depicted in Fig. 2.

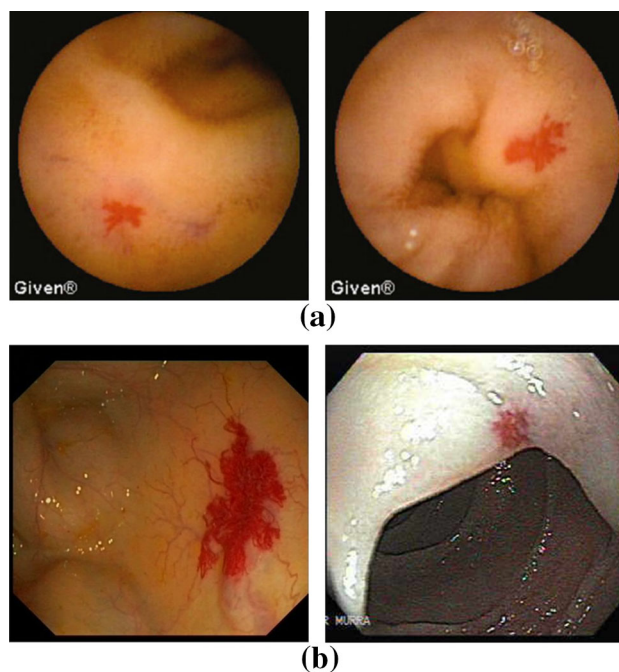


Fig. 1 Example images of angiectasia lesions. Dilation of mucosa capillaries causes a reticular or fernlike pattern. **a** Capsule endoscopic images [1]; **b** Wired white light endoscopic images [31], [24]

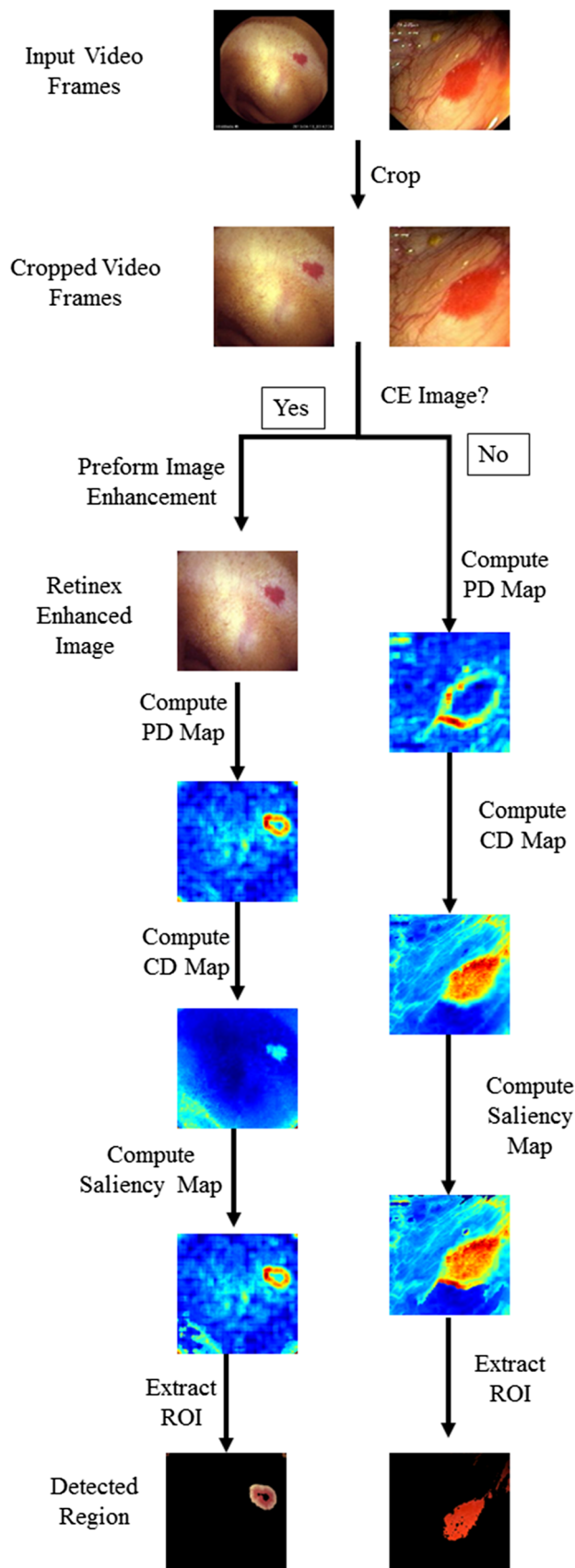


Fig. 2 An overview of the proposed system. A common approach is adopted for both wired and capsule endoscopic (CE) images. However, for CE images, image enhancement using Retinex is performed to achieve comparable illumination to wired endoscopic images. Saliency detection algorithm has been applied on the pre-processed images. Saliency detection algorithm includes three steps: computing the pattern distinctness (PD) map, computing the color distinctness (CD) map, and combining PD and CD maps to form saliency map. Finally, adaptive thresholding is performed on the saliency map for the localization and detection of angiectasia

2.1 Pre-processing

The border edges in the endoscopic images can interfere in saliency computation. To remove the boundary effect, we perform image cropping discarding the black background.

To enable the application of same saliency detection algorithm for both capsule and wired endoscopic images, an adaptive image enhancement method based on Retinex theory is applied on the capsule endoscopic images [16]. The capsule endoscopic images suffer from inhomogeneous brightness, poor contrast and different artifacts due to the uncontrolled motion of the capsule and dynamic illumination condition in the absence of ambient light. In Fig. 3a and e, we can see the difference in illumination condition between capsule and wired endoscopic images. Retinex theory, based on color constancy phenomenon, compensates for non-uniform illumination effect in images. Color constancy refers to the human visual system characteristics where the observer can recognize and match color under a wide range of different illumination. The Retinex theory uses this property to extract the reflectance and illumination image from the input image [17, 18]. Previous research shows that Retinex theory can improve the image quality and additionally enhances the saliency of capsule endoscopic images [19]. Therefore, in this work, we have applied the Retinex theory on capsule endoscopic images to extract and enhance the illumination image to achieve comparable illumination in capsule endoscopic images as wired endoscopic images.

According to Retinex theory, an input image $I(x, y)$ can be expressed as:

$$I(x, y) = L(x, y) \cdot R(x, y) \quad (1)$$

where $L(x, y)$ and $R(x, y)$ are respectively the illumination image and the reflectance image. A variational framework has been adopted to compute the illumination image [16], [17] by minimizing the following cost function:

$$F(l) = \int \left(|\nabla l|^2 + \alpha(i - l)^2 + \beta|\nabla(i - l)^2| \right) dx dy \quad (2)$$

where α and β are parameters, $i(x, y)$ and $l(x, y)$ represent the logarithm of input image and illumination image.

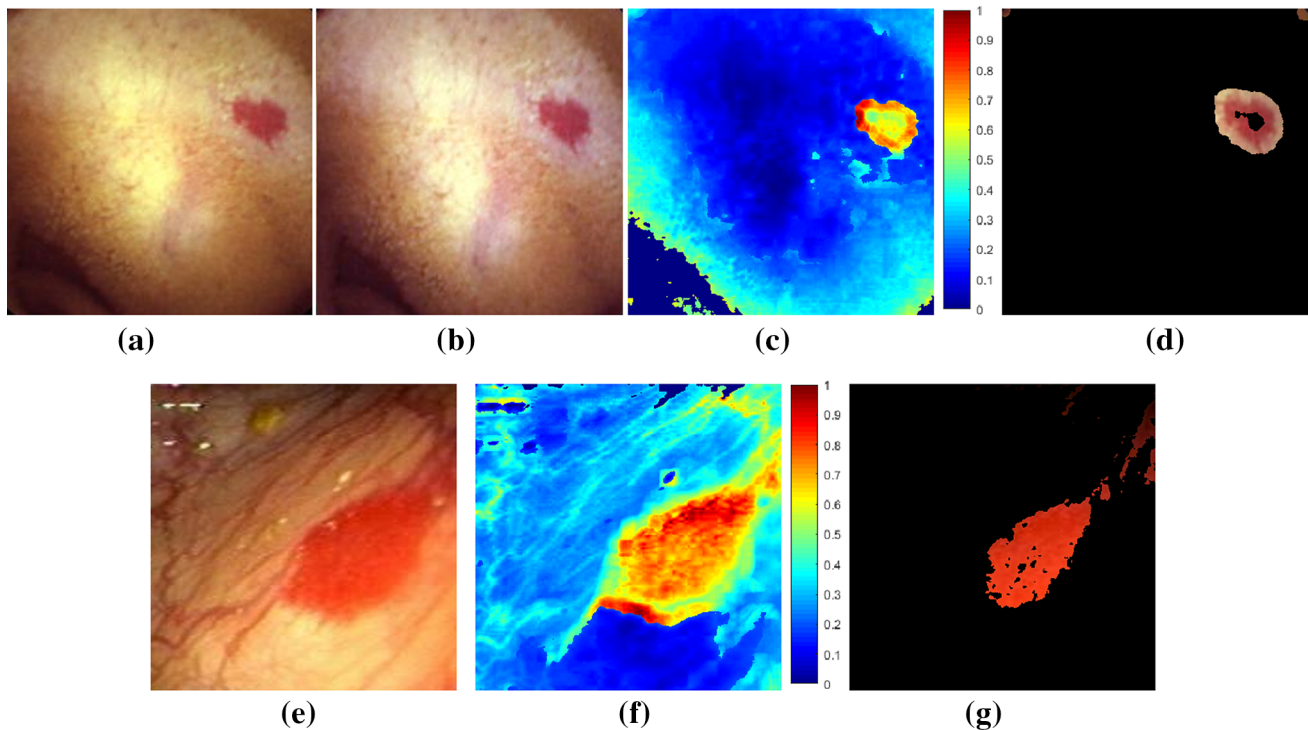


Fig. 3 Effect of applying different stages of the algorithm on two example images. **a** capsule endoscopic (CE) image example; **b** CE image after applying Retinex; **c** Saliency map obtained combining CD map and PD map from the CE image; **d** final detection after applying

adaptive thresholding from the CE image, **e** wired endoscopic image example; **f** Saliency map obtained combining CD map and PD map from the wired endoscopic image; **g** final detection after applying adaptive thresholding from the wired endoscopic image

After obtaining the logarithm of illumination image $l(x, y)$, the reflectance image is obtained by:

$$R = \exp(i - l) \quad (3)$$

The illumination image $L(x, y)$ is then adjusted to obtain comparable illumination to wired endoscopic image:

$$L' = L^\gamma \quad (4)$$

The final enhanced image is obtained by using:

$$I' = L' \cdot R \quad (5)$$

Figure 3 shows the effect of enhancement achieved using Retinex algorithm. We can see that the preprocessing scheme was able to improve illumination condition in the capsule endoscopic image.

2.2 Saliency Detection Algorithm

We propose an unsupervised saliency detection algorithm, which captures the distinguishing characteristic of angiectasia. A region containing angiectasia is different both in pattern and color compared to the neighboring image patches. Therefore, we define a pattern distinctness (PD) measure and a color distinctness (CD) measure and integrate them to distinguish angiectasia regions.

2.2.1 Pattern Distinctness

We have adopted the method proposed in [20] to compute a patch distinctness (PD) map. Patch distinctness map identifies the salient regions in the endoscopic image. Pattern distinctness is measured by comparing each image patch to the average patch. A patch which is dissimilar to the average patch is considered to be salient. A computationally efficient way to compare the image patches to the average patch has been proposed in [20], where the image patches are represented by corresponding principle components obtained through Principle component analysis (PCA) and the distance of the image patches from the average patch are computed by summing up the projections along the principle axis. According to the proposed method in [20], an input image is first divided into $k \times k$ overlapping patches. For each patch p_x , PCA gives a set of principle components a_k^x which defines the coordinate \tilde{p}_x of the corresponding patch in the PCA coordinate system. Then the patch distinctness for the patch p_x centered at pixel x is given as:

$$P(x) = \|\tilde{p}_x\|_1 = \sum_k |a_k^x| \quad (6)$$

Figure 6 shows example endoscopic images and the corresponding PD maps. Angiectasia affected regions are

found to be more emphasized compared to the normal regions in the PD map.

2.2.2 Color Distinctness

The angiectasia lesions are distinct from the normal mucosa with their characterizing reddish hue. The index of hemoglobin (IHb) is a measure of the hemoglobin content in gastrointestinal mucosa [21]. IHb index has been found to be useful in distinguishing between adenoma and normal mucosa [21, 22]. However, IHb has not been applied to distinguish between normal and angiectasia regions in previous works. In our experiments, we found strong correlation between IHb index and presence of angiectasia. The IHb index was calculated using the following equation:

$$IHb(x) = 32 \times \log_2 \left(\frac{R(x)}{G(x)} \right) \quad (7)$$

Here, $R(x)$ and $G(x)$ are the red and green channel values of the endoscopic image pixels. We define IHb index to be a color distinctness measure to distinguish between normal and angiectasia regions. We propose the computation of color distinctness (CD) map based on the color distinctness measure. Figure 5 shows example endoscopic images and the corresponding CD maps. The images show that angiectasia affected regions are highlighted in the CD map.

2.2.3 Saliency Map Formation

Both PD map and CD map emphasize the regions containing angiectasia, along with a few normal regions. To extract the regions which are salient in both color and pattern, we combine the PD map and CD map to form the final saliency map:

$$S(x) = P(x) \cdot IHb(x) \quad (8)$$

The final saliency map is normalized to the range [0, 1]. Figure 3c and f demonstrate final saliency maps for example capsule endoscopy image and wired endoscopic image respectively, where it can be seen that angiectasia affected regions are significantly distinguished from the normal regions by means of higher saliency value.

2.3 ROI Localization Using Adaptive Thresholding

We propose a region-of-interest (ROI) localization algorithm based on adaptive thresholding. First, we compute the gradient image from the saliency map. From the gradient image, we can see that the peak in the saliency map (associated with gradient zero) are surrounded by a region with gradually decreasing saliency score. From the gradient image, we extract all the peaks (i.e. modes of the saliency

map) with saliency score greater than a threshold, T_{\max} . To extract the regions-of-interest around the peak, we perform local thresholding around the peak with a threshold value, T . Figure 3d and g demonstrate the ROI localization performance for an example capsule endoscopy image and wired endoscopic image, respectively,

3 Experimental Results

Experimental results are carried out to measure the effectiveness of each stage and the overall algorithm in detecting angiectasia. All the experiments were performed using MATLAB 2015a (The MathWorks Inc., Natick, Massachusetts, USA). This section provides detail description of the experiment and discussion on the performance.

3.1 Data Description

The proposed algorithm is designed to detect angiectasia in both capsule and wired white-light endoscopic images. Therefore, for performance evaluation, we create a database containing images extracted from both modalities. We have collected 4 CE (frame rate = 2 fps) and 5 wired endoscopic video clips (frame rate = 30 fps) containing angiectasia and 5 CE and 5 wired endoscopic video containing normal images from the publicly available databases [23, 24]. In total, our result is based on 3602 video frames among which 968 frames contain angiectasia. All the video frames were resized to dimension of 256×256 . Table 1 gives a description of data used in our experiments.

3.2 Performance Metrics

An important aspect of the proposed algorithm is its capability to localize the ROI by detecting a significant portion of the affected region, in contrary to previous detection algorithm where an abnormality is considered to be detected even if a single point belonging to the abnormality is detected [14, 25]. Another important criterion for an effective detection system is to generate minimum false alarms in order to reduce the number of frames requiring manual inspection. Therefore, we evaluate the performance of the algorithm based on two criteria: (i) angiectasia localization and (ii) angiectasia detection.

3.2.1 Angiectasia Localization

An angiectasiac lesion will be considered to be detected if the area of overlap between the detected region and the ground truth region exceeds 50%.

Table 1 Description of experimental data

Image acquisition mode	Angiectasia		Normal	
	Video clip	Video frame	Video clip	Video frame
Wired endoscopy	5	914	5	2292
Capsule endoscopy	4	54	5	342
Total	9	968	10	2634

$$overallp = \frac{b_{detected} \cap b_{groundtruth}}{b_{detected} \cup b_{groundtruth}} \quad (9)$$

Localization performance is evaluated on images containing angiectasia (excluding images with normal pathologies). The metrics for evaluating localization performance are:

- Localization Score measures the fraction of correctly detection regions compared to the total angiectasiac regions.

$$Localization\ Score = \frac{TP}{TP + FN} \quad (10)$$

TP is the number of correctly detected regions which satisfy the overlap criteria, whereas FN is the number of angiectasiac regions which have not been detected or the detection does not meet the overlap criteria.

- Localization Precision measures the fraction of correctly detection regions among the total detected regions in frames containing angiectasia.

$$Localization\ Precision = \frac{TP}{TP + FP} \quad (11)$$

FP is the number of incorrectly detected regions in the frames containing angiectasia.

3.2.2 Angiectasia Detection

Detection performance is evaluated on the entire dataset containing both angiectasia and normal pathologies. The following metric was adopted for evaluating angiectasia detection:

- Detection Latency: Detection latency is defined as the time from the first appearance of an abnormality in endoscopic video to time of its first detection by the proposed method.

$$Detection\ Latency = \frac{Frame\ Number\ where\ angiectasia\ first\ detected - Frame\ Number\ where\ angiectasia\ first\ appears}{frame\ rate}$$

Detection latency was first proposed in [26] in context of polyp detection. However, this measure is very relevant to angiectasia detection, especially in case of capsule

endoscopic videos where only a few frames might contain the lesion. Nevertheless, latency is also important for wired endoscopic videos as it can signal the presence of a subtle lesion allowing the physician to perform detail examination, which otherwise could have been missed.

3.3 Effectiveness of PD and CD Measures

Both PD and CD measures have important role to form a saliency map distinguishing angiectasiac regions from the normal mucosa. To demonstrate the efficacy of these measures, box-whisker plot showing CD and PD values for normal and angiectasia regions has been given in Fig. 4. The plots are based on smaller dataset containing 100 angiectasiac images. The PD and CD values are taken as the mean of angiectasiac and normal regions from each image of the dataset. Figure 4a shows that the values of IHB indices have large separation for angiectasiac and normal regions. Angiectasiac regions have significantly higher IHB value compared to normal regions. On the other hand, PD measures also show reasonable separation, however, with slight overlapping in case of outlier examples (Fig. 4b). Figure 5 gives visual demonstration of CD measures in distinguishing angiectasia compared to normal regions. CD measures are single-handedly capable to highlight the angiectasiac regions in both capsule and wired endoscopic images. Although, mucosal folds, dark lumen also have high IHB indices and are highlighted in CD map. Figure 6 qualitatively shows the efficacy of PD measures in angiectasia detection. In case of large angiectasiac regions (often seen in wired endoscopic videos due to close-up image acquisition), lesions are only partially detected. The underlying reason is that the lesion patches are more similar to the average patch as the average patch is dominated by the patches containing

lesion. Therefore, these patches do not qualify as distinct. However, combining the CD and PD maps, the limitation of each measure can be overcome.

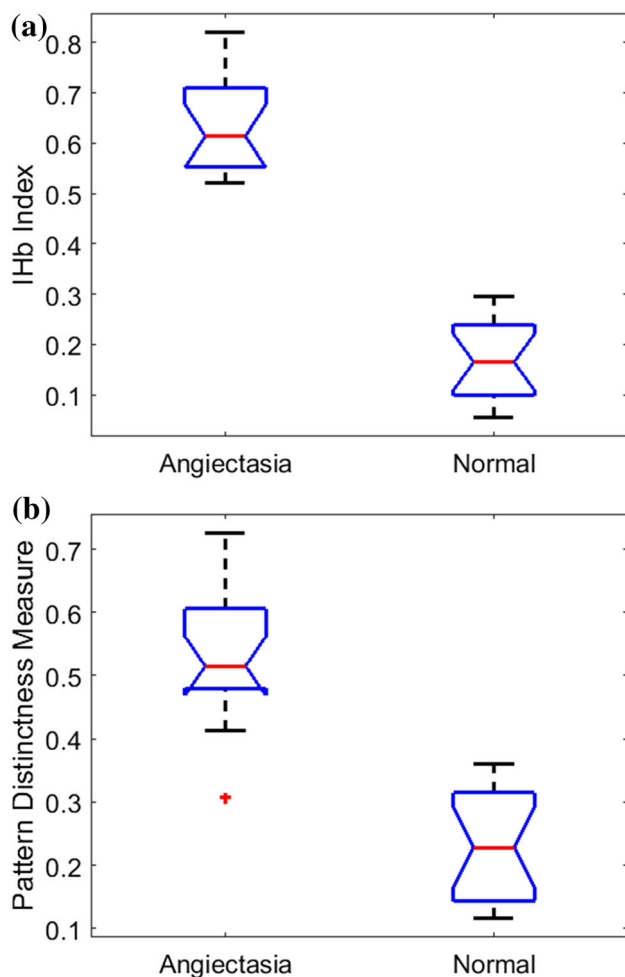


Fig. 4 Box-whisker plot exhibiting variation between (a) IHb indices and (b) PD measures for angiectasia affected and normal regions

3.4 Performance Evaluation

This section provides the performance evaluation of the proposed method in terms of angiectasia localization and angiectasia detection. Table 2 shows the angiectasia localization performance. From the table, it can be realized that in capsule endoscopic videos, only a few frames contain angiectasia. Therefore, it is difficult to collect large number of frames containing angiectasia. For capsule endoscopic videos, it is crucial to design a detection method with very high sensitivity and minimum detection latency. Otherwise, these lesions could have gone undetected in clinical application. It is evidenced from Table 2 that the proposed system has very high sensitivity to angiectasia and very low detection latency. On the other hand, wired endoscopy provides the option for manual controlling of the probe for better visualization. Therefore, a lesion can be found in numerous video frames with different viewing angle and distance, once it is found by the physician. However, there is a chance of missing a lesion if

initially the physician fails to detect the presence due to fatigue or minute appearance of the lesion. In this case, our proposed method has shown excellent performance to detect angiectasiac lesions with a very short detection latency. The high localization score and localization precision suggest that the proposed algorithm can serve as an alternative to manual screening or an additional viewer ensuring higher detection performance.

Another major aspect of an effective detection system is to minimize the number of false positive events. Especially, capsule endoscopy gives rise to 50,000–72,000 frames per patient with only a few frames containing clinically significant regions [27]. An effective CAD system with a few false positive events can significantly reduce the number of frames requiring the attention of the physician. Table 3 shows that the proposed system can reduce the number of frames by more than 80%.

3.5 Performance Comparison

The proposed angiectasia detection algorithm is based on saliency map formation. Therefore, we compare the localization performance of our proposed method with three state-of-the-art saliency detection algorithms: HSSR [28], GBVS [29], and SBVA [30]. A visual demonstration of the localization performance for each of these methods including our proposed method has been given in Fig. 7. The column (a) shows the original images, (b) shows the corresponding ground truth images, and (c) to (f) show the estimated saliency maps obtained using HSSR [28], GBVS [29], SBVA [30], and our method. From this figure, it is clearly visible that the saliency detection algorithm designed for natural images are not suitable to detect angiectasia in most cases. Rather the traditional saliency detection methods detect visual salient region, for example, mucosa folds, specular reflection, bubble, etc. On the other hand, the proposed saliency detection method specific to angiectasia successfully localizes the affected regions. Table 4 presents a quantitative comparison among the methods. The table is based on a subset of 50 images, including both capsule and traditional endoscopic images, taken from the entire dataset. The threshold parameter for each method was empirically chosen to obtain the best localization performance. From the table, it can be seen that our proposed method outperforms the state-of-the-art saliency detection algorithms requiring significantly less computational time.

4 Conclusion

This paper identifies angiectasia detection as an individual computer-aided detection problem and presents a novel, efficient and computationally simple method dedicated for

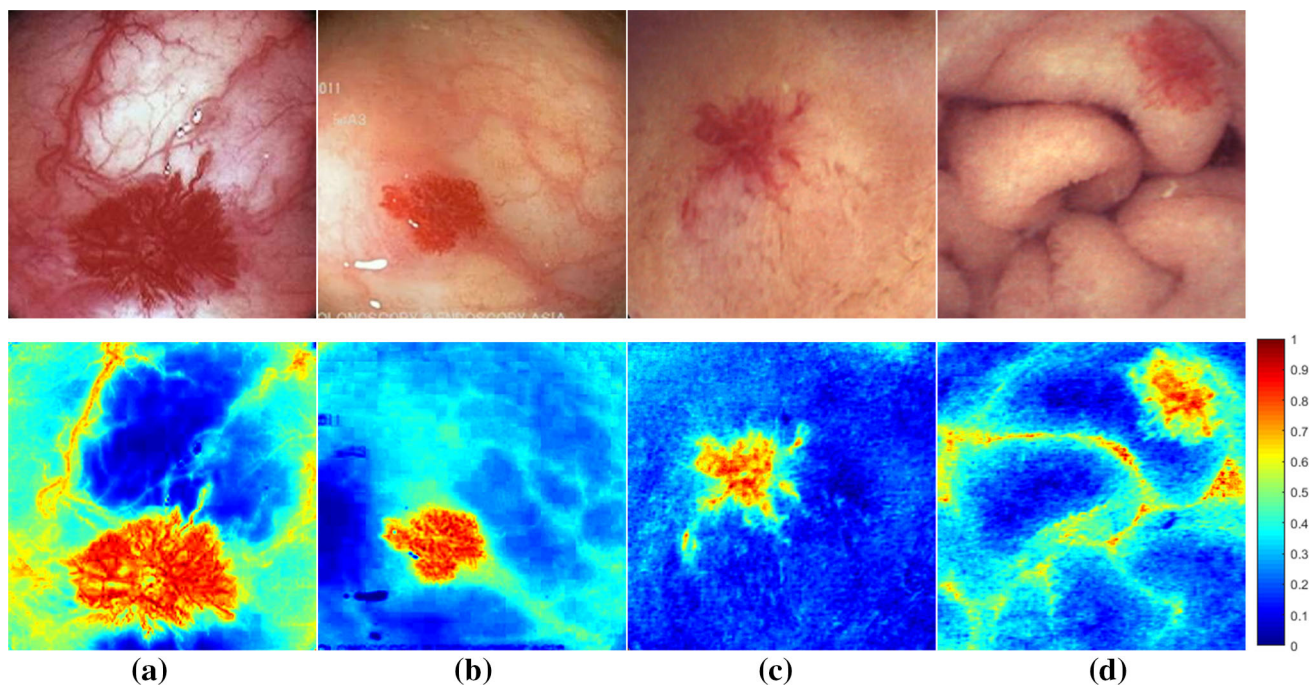


Fig. 5 Color distinctness (CD) map for endoscopic images. *Top*: original images. *Bottom*: CD map. **a** and **b** show wired endoscope images and **c** and **d** show capsule endoscopic images. Angiectasia

affected regions are highlighted in all the images, however, regions with mucosal fold in capsule endoscopic images tend to have high IHb indices

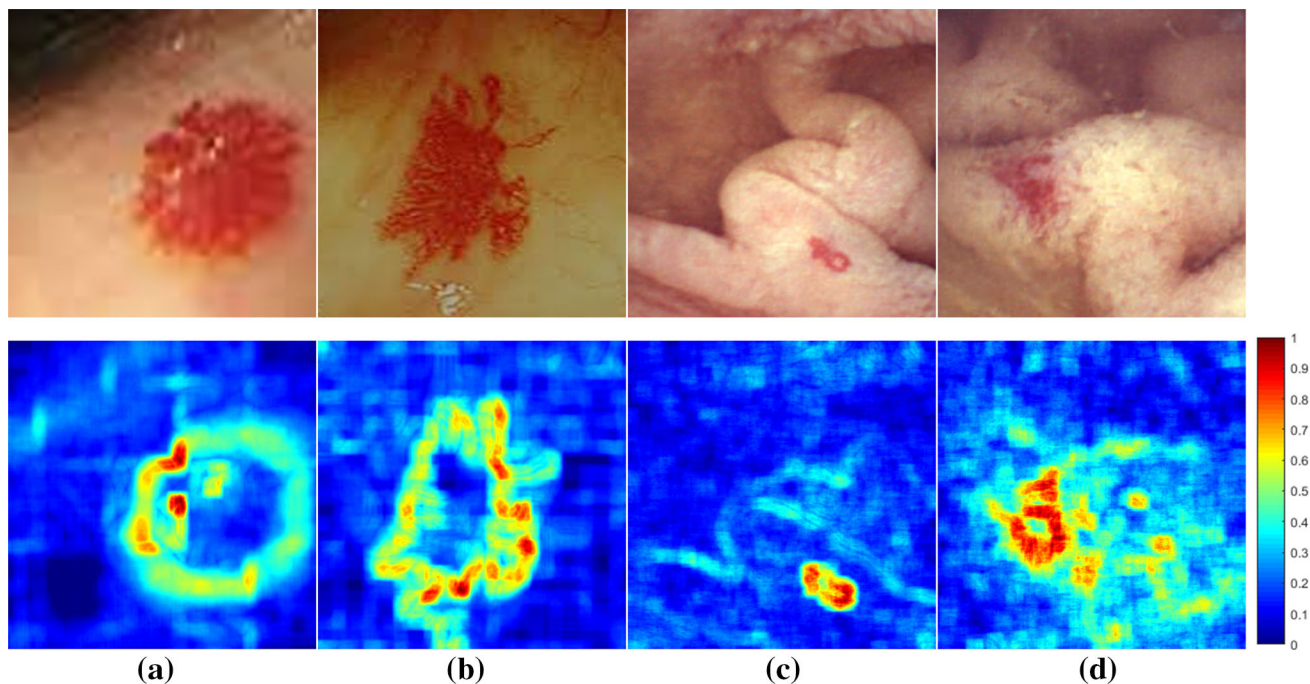


Fig. 6 Pattern distinctness (PD) map for wired endoscopic images (**a** and **b**) and for capsule endoscopic images (**c** and **d**). *Top*: original images. *Bottom*: PD map. Beside angiectasia affected regions, other salient region, e.g., specular reflection, bubble are also highlighted

angiectasia localization and detection. Angiectasia, with presence in a few images and posing significant economic burden as a primary cause of obscure GI bleeding (OGIB),

is a challenging health issue to physicians. The proposed method can play a major role to aid the physician by improving angiectasia detection rate. The unsupervised

Table 2 Angiectasia localization performance

Video		GT	TP	FP	FN	Loc. Score (%)	Loc. Prec. (%)	Latency (s)
Wired	Video 1	164	152	39	12	92.68	79.58	0.13
	Video 2	273	265	16	8	97.06	94.3	0
	Video 3	66	56	3	10	84.85	94.92	0.17
	Video 4	199	188	15	11	94.45	92.61	0.03
	Video 5	212	208	7	4	98.11	97.64	0
	Total	914	869	80	45	95.08	91.57	N/A
Capsule	Video 6	3	3	2	0	100	69	0
	Video 7	5	4	0	1	80	100	0.03
	Video 8	8	7	4	1	87.5	63.64	0.03
	Video 9	38	37	2	1	97.36	94.87	0
	Total	54	51	8	3	94.44	86.44	N/A

Table 3 Angiectasia detection performance

Image acquisition mode	Sensitivity (%)	Specificity (%)
Wired endoscopy	95.08	80.77
Capsule endoscopy	94.44	83.92

method does not require any prior training. This is a desirable aspect for detection method as its performance will not depend on the size and quality of training data. We have performed extensive experiments with a large dataset containing a total of 3602 images, among which 968

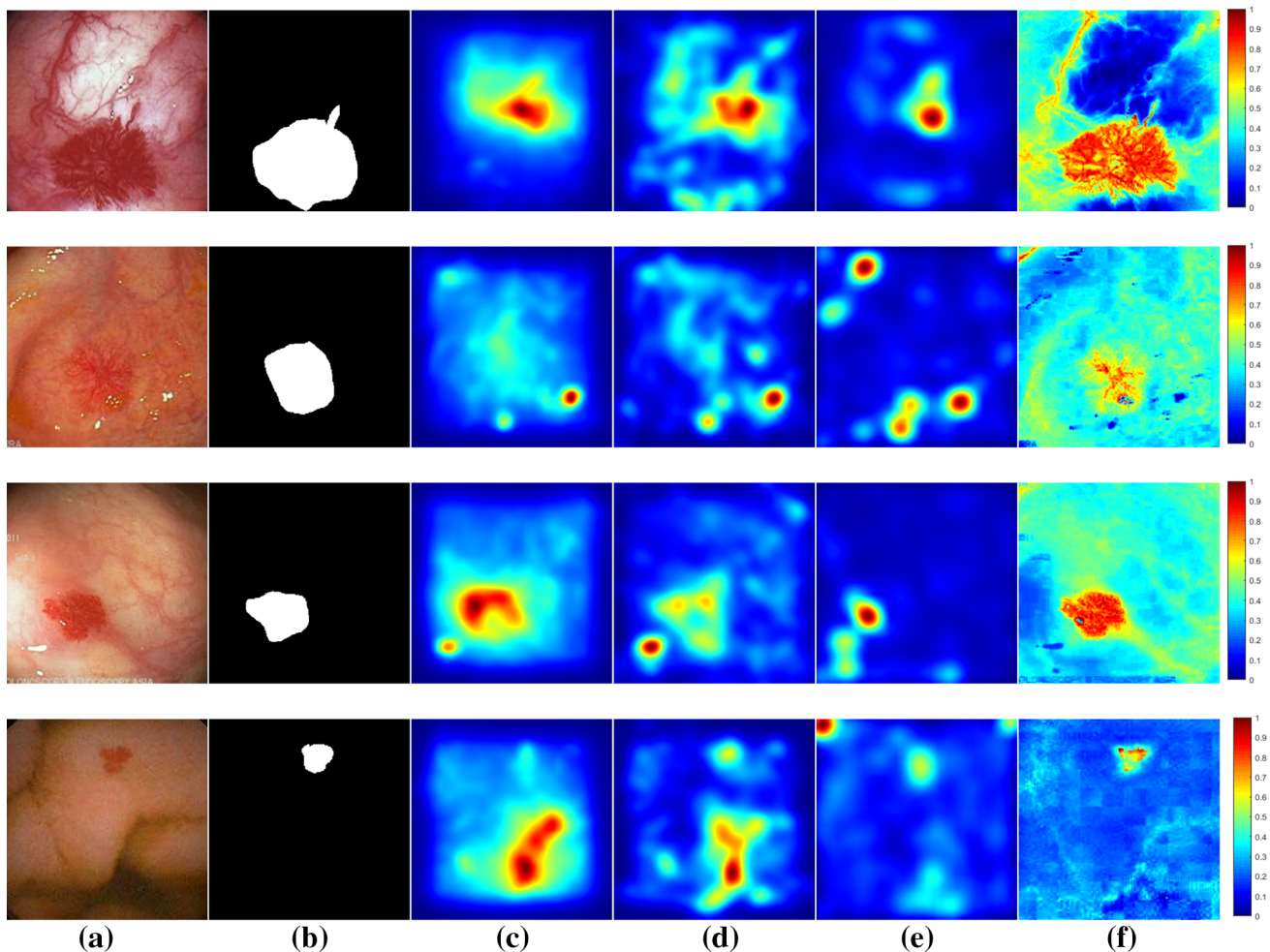


Fig. 7 Qualitative comparison of angiectasia localization performance obtained using HSSR [28], GBVS [29], SBVA [30], and our method. **a** Original image, **b** ground-truth image, **c** saliency map

formed using HSSR [28], **d** saliency map formed using GBVS [29], **e** saliency map formed using SBVA [30], **f** saliency map formed using proposed method

Table 4 Performance comparison with state-of-the-art saliency detection algorithms

Method	Overlap ($\mu \pm \sigma$)	Localization score (%)	Computation time (s)
HSSR [28]	0.0992 \pm 0.23	42.1	1.3525
GBVS [29]	0.1449 \pm 0.2	52.63	0.7845
SBVA [30]	0.0538 \pm 0.09	26.32	0.1765
Proposed	0.4663 \pm 0.2257	95.04	0.02

Bold values represent best performances

images contain angiectasia. Our method is applicable for both wired and capsule endoscopic video frames. For both modalities, excellent localization performance has been achieved. The detection latency for CE images is less than 0.1 s and for wired endoscopic images is less than 0.2 s. Besides achieving very high sensitivity ($\approx 95\%$), the method also results in moderately high specificity ($>80\%$). Therefore, the number of frames requiring manual viewing can be reduced by 80%. The unsupervised detection algorithm is based on saliency detection algorithm, which is specifically designed to detect angiectasia. The proposed saliency detection algorithm significantly outperforms the state-of-the-art saliency detection algorithms, requiring less computational time. The algorithm can be further improved by considering the distinct shape of the angiectasiac regions. In future, we will investigate the possibility of including the shape distinctness of angiectasia in saliency map formation for improving the angiectasia detection performance.

References

- Keuchel, M., Hagenmüller, F., & Tajiri, H. (2014). *Video capsule endoscopy: A reference guide and atlas*. Berlin: Springer.
- Höög, C. M., Broström, O., Lindahl, T. L., Hillarp, A., Lärfars, G., & Sjöqvist, U. (2010). Bleeding from gastrointestinal angiectasias is not related to bleeding disorders—a case control study. *BMC gastroenterology*, *10*(1), 113.
- Raju, G. S., Gerson, L., Das, A., & Lewis, B. (2007). American Gastroenterological Association (AGA) Institute Technical Review on Obscure Gastrointestinal Bleeding. *Gastroenterology*, *133*(5), 1697–1717.
- Cúrdia Gonçalves, T., Magalhães, J., Boal Carvalho, P., Moreira, M. J., Rosa, B., & Cotter, J. (2014). Is it possible to predict the presence of intestinal angiectasias? *Diagnostic and therapeutic endoscopy*. doi:10.1155/2014/461602.
- Bollinger, E., Raines, D., & Saitta, P. (2012). Distribution of bleeding gastrointestinal angiectasias in a Western population. *World Journal of Gastroenterology*, *18*(43), 6235–6239.
- Gunjan, D., Sharma, V., Rana, S. S., & Bhasin, D. K. (2014). Small bowel bleeding: A comprehensive review. *Gastroenterology Report*, *2*(4), 262–275.
- Sami, S. S., Al-Araji, S. A., & Ragunath, K. (2014). Review article: Gastrointestinal angiodysplasia-pathogenesis, diagnosis and management. *Alimentary Pharmacology & Therapeutics*, *39*(1), 15–34.
- Iakovidis, D. K., & Koulaouzidis, A. (2015). Software for enhanced video capsule endoscopy: Challenges for essential progress. *Nature Reviews Gastroenterology & Hepatology*, *12*(3), 172–186.
- Liedlgruber, M., & Uhl, A. (2011). Computer-aided decision support systems for endoscopy in the gastrointestinal tract: A review. *IEEE Reviews in Biomedical Engineering*, *4*, 73–88.
- Yuan, Y., Li, B., & Meng, Q. (2016). Bleeding frame and region detection in the wireless capsule endoscopy video. *IEEE Journal Biomedical and Health Informatics*, *20*(2), 624–630.
- Iakovidis, D. K., Chatzis, D., Chrysanthopoulos, P., & Koulaouzidis, A. (2015). Blood detection in wireless capsule endoscopy images based on salient superpixels. In: *37th Annual International Conference of the IEEE, Engineering in Medicine and Biology Society (EMBC)*, (pp. 731–734).
- Yuan, Y., Wang, J., Li, B., & Meng, M. (2015). Saliency based ulcer detection for wireless capsule endoscopy diagnosis. *IEEE Transactions on Medical Imaging*, *34*(10), 2046–2057.
- Deeba, F., Mohammed, S. K., Bui, F., & Wahid, K. (2017). Efficacy evaluation of save for the diagnosis of superficial neoplastic lesion. *IEEE Journal of Translational Engineering in Health and Medicine*. doi:10.1109/JTEHM.2017.2691339.
- Iakovidis, D. K., & Koulaouzidis, A. (2014). Automatic lesion detection in capsule endoscopy based on color saliency: Closer to an essential adjunct for reviewing software. *Gastrointestinal Endoscopy*, *80*(5), 877–883.
- Stockman, D. L. (2016). *Diagnostic pathology: Vascular*. Netherland: Elsevier.
- Okuhata, H., Nakamura, H., Hara, S., Tsutsui, H., & Onoye, T. (2013). Application of the real-time Retinex image enhancement for endoscopic images. In: *2013 35th Annual International Conference of the IEEE, Engineering in Medicine and Biology Society (EMBC)*, pp. 3407–3410.
- Kimmel, R., Elad, M., Shaked, D., Keshet, R., & Sobel, I. (2003). A variational framework for retinex. *International Journal of Computer Vision*, *52*(1), 7–23.
- Land, E. H. (1977). The retinex theory of color vision. *Scientific American*, *237*, 108–128.
- Deeba, F., Mohammed, S. K., Bui, F. M., & Wahid, K. A. (2016). Unsupervised Abnormality Detection Using Saliency and Retinex based Color Enhancement. In: *The 38th Annual International Conference of the IEEE Engineering in Medicine and Biology Society*, pp. 3871–3874.
- Margolin, R., Tal, A., & Zelnik-Manor, L. (2013). What makes a patch distinct?. In: *Proceedings of IEEE Computer Society Conference Computer Vision Pattern Recognition*, 1139–1146.
- Cheng, W. C., Cheng, H. C., Chen, P. J., Kang, J. W., Yang, E. H., Sheu, B.-S., et al. (2015). Higher net change of index of hemoglobin values between colon polyp and nonpolyp mucosa correlates with the presence of an advanced colon adenoma. *Advances in Digestive Medicine*. doi:10.1016/j.aidm.2015.04.005.
- Kobayashi, K., Igarashi, M., Sada, M., Katsumata, T., & Saigenji, K. (2002). Clinical significance of adaptive index of hemoglobin color enhancement for endoscopic diagnosis of superficial type colorectal tumors. *Digestive Endoscopy*, *14*(s1), S51–S53.
- CapsuleEndoscopy.org. Retrieved from <http://www.capsuleendoscopy.org/Pages/default.aspx>.

24. El Atlas Gastrointestinal. Retrieved from <http://www.gastrointestinalatlas.com/>.
25. Sainju, S., Bui, F. M., & Wahid, K. A. (2014). Automated bleeding detection in capsule endoscopy videos using statistical features and region growing. *Journal of Medical Systems*, 38(4), 25.
26. Tajbakhsh, N., Gurudu, S. R., & Liang, J. (2016). Automated polyp detection in colonoscopy videos using shape and context information. *IEEE Transactions on Medical Imaging*, 35(2), 630–644.
27. Koulaouzidis, A., Rondonotti, E., & Karargyris, A. (2013). Small-bowel capsule endoscopy: A ten-point contemporary. *World Journal of Gastroenterology*, 19(24), 3726–3746.
28. Hou, X., Harel, J., & Koch, C. (2012). Image signature: Highlighting sparse salient regions. *IEEE Transactions on Pattern Analysis and Machine Intelligence*, 34(1), 194–201.
29. Harel, J., Koch, C., & Perona, P. (2007). Graph-based visual saliency. In *Advances in neural information processing systems*, 545–552.
30. Itti, L., Koch, C., & Niebur, E. (1998). A model of saliency-based visual attention for rapid scene analysis. *IEEE Transactions on Pattern Analysis and Machine Intelligence*, 20(11), 1254–1259.
31. WEO Clinical Endoscopy Atlas (2014). <http://www.endoatlas.org/>. Accessed 25 May 2016.